Biosensors and Bioelectronics 294 (2026) 118182

Contents lists available at ScienceDirect

Biosensors and Bioelectronics

journal homepage: www.elsevier.com/locate/bios

A colorimetric strategy for quantifying amino acids using *E. coli* auxotrophs displaying gold-binding proteins

Hee Tae Ahn [a,1], Byung Jo Yu [b,1], Thinh Viet Dang [a], Soobin Lee [c], In Seung Jang [b], Dong Hoon Lee [a], Tae Jung Park [d], Moon Il Kim [a,*], Hyun Gyu Park [c,**]

[a] Department of BioNano Technology, Gachon University, 1342 Seongnamdae-ro, Sujeong-gu, Seongnam, Gyeonggi, 13120, Republic of Korea
[b] Low-Carbon Transition R&D Department, Research Institute of Sustainable Development Technology, Korea Institute of Industrial Technology (KITECH), Cheonan, 31056, Republic of Korea
[c] Department of Chemical and Biomolecular Engineering (BK21 Four), Korea Advanced Institute of Science and Technology (KAIST), 291 Daehak-ro, Yuseong-gu, Daejeon, 34141, Republic of Korea
[d] Department of Chemistry, Research Institute of Chem-Bio Diagnostic Technology, Chung-Ang University, 84 Heukseok-ro, Dongjak-gu, Seoul, 06974, Republic of Korea

ARTICLE INFO

Keywords:
Escherichia coli auxotroph
Gold-binding protein
Amino acid detection
Colorimetric biosensor

ABSTRACT

We present a cell-based colorimetric assay for amino acid quantification using *Escherichia coli* auxotrophs engineered to grow exclusively in the presence of their corresponding target amino acids and to display gold-binding proteins (GBPs) on their surface. Upon the addition of gold nanoparticles (AuNPs), the surface-expressed GBPs mediate AuNP aggregation, resulting in a distinct color shift from pink to blue. This approach enables the detection of ten essential amino acids through characteristic colorimetric changes and allows for quantitative analysis via absorbance measurements with high specificity, strong linearity ($R^2 > 0.96$), and low detection limits ranging from 0.43 to 1.04 μM. The clinical applicability of the assay was demonstrated by accurately detecting elevated amino acid levels associated with phenylketonuria (PKU), homocystinuria, and maple syrup urine disease (MSUD), with excellent analytical precision (coefficients of variation <4 %) and high recovery rates (98–102 %). This technology holds strong potential as a novel platform for amino acid quantification, providing an easily observable colorimetric readout without the need for bulky or specialized instrumentation.

1. Introduction

Amino acids are the fundamental building blocks of proteins and are indispensable for nearly all biochemical and physiological processes in living organisms (Häusler et al., 2014; Kaur et al., 2023). Abnormal concentrations of amino acids can disrupt normal metabolic pathways, leading to physiological dysfunctions and various metabolic disorders (Han et al., 2023; Zhang et al., 2024). Among the twenty standard amino acids, ten are classified as essential because they cannot be synthesized endogenously and must therefore be obtained through dietary intake (Hou et al., 2015; Kaur et al., 2023).

The precise quantification of these essential amino acids is particularly crucial for monitoring nutritional status and diagnosing inherited metabolic disorders which often manifest in newborn babies (Yahyaoui and Pérez-Frías, 2019). Conditions such as phenylketonuria (PKU), homocystinuria, and maple syrup urine disease (MSUD) arise from genetic defects in amino acid metabolism pathways and can lead to severe developmental complications, neurological disorders, and other life-threatening conditions, if not detected and treated early (Aliu et al., 2018; Chen et al., 2023; Garg and Dasouki, 2006; Kilgore et al., 2023; Matuszewska et al., 2024; Shykholeslami et al., 2022). Therefore, developing accurate and accessible amino acid quantification methods is critical for the early diagnosis of these disorders, especially in newborn screening and timely clinical management.

Current approaches for amino acid quantification primarily depend on sophisticated instrumental techniques such as high-performance

This article is part of a special issue entitled: SynBio-based Biosensors published in Biosensors and Bioelectronics.

* Corresponding author.
** Corresponding author.
E-mail addresses: moonil@gachon.ac.kr (M.I. Kim), hgpark@kaist.ac.kr (H.G. Park).
[1] These authors contributed equally to this work.

https://doi.org/10.1016/j.bios.2025.118182
Received 6 August 2025; Received in revised form 14 October 2025; Accepted 30 October 2025
Available online 31 October 2025

liquid chromatography (HPLC) and mass spectrometry (Bouza et al., 2024; Giordano et al., 2019; Kaur et al., 2023; Xie et al., 2022). While these methods offer outstanding analytical performance, their practical utility is often hindered by several limitations, including the high cost of instrumentation, the requirement for specialized expertise, and labor-intensive sample preparation procedures. These constraints are especially prohibitive in decentralized or resource-limited environments. Consequently, there is a growing need for alternative platforms that enable cost-effective and user-friendly amino acid detection without compromising analytical quality.

Cell-based biosensors have emerged as compelling alternatives to conventional analytical methods due to their reduced operational complexity and cost (Chung and Dhar, 2021; Gupta et al., 2019; Kannappan and Ramisetty, 2022; Lu et al., 2021). Among these, *E. coli* auxotroph-based biosensors show strong potential for amino acid quantification by utilizing strains that grow exclusively in the presence of specific target amino acids (Bertels et al., 2012; Kang et al., 2022). Our group has pioneered this approach by engineering auxotrophic *E. coli* strains harboring luminescent or fluorescent reporter systems, enabling selective and quantitative detection of amino acids and related metabolites, including homocysteine and galactose (Kim et al., 2010, 2014; Woo et al., 2011, 2013). Extending our earlier research, we further enhanced the platform by incorporating gold-binding protein (GBP)-displaying plasmids into leucine auxotrophic *E. coli*, allowing for leucine quantification relevant to the diagnosis of MSUD, based on surface plasmon resonance (SPR) signals generated through specific interactions between cell-surface GBPs and gold-coated SPR chips (Woo et al., 2016).

Building upon our previous work, we present a colorimetric biosensor platform for the simultaneous detection of ten essential amino acids. This system integrates auxotrophic *E. coli* strains with the plasmid pTacFadLGBP-1, enabling surface expression of GBPs in proportion to target amino acid concentrations (Park et al., 2009). GBP-mediated aggregation of gold nanoparticles (AuNPs) induces a visible pink-to-blue color shift, allowing both qualitative and quantitative analysis without the need for complex instrumentation. We demonstrate the clinical relevance of this platform by detecting elevated levels of phenylalanine, methionine, and leucine in dried spot samples containing pathologically relevant amino acid concentrations. This work represents a significant advance toward simple, accessible, and scalable diagnostics for amino acid-related diseases.

2. Experimental section

2.1. Construction of GBP-displaying E. coli auxotrophs

E. coli auxotrophic strains for ten essential amino acids—arginine, histidine, isoleucine, leucine, lysine, methionine, phenylalanine, threonine, tryptophan, and valine—were generated via transposon mutagenesis using a previously established protocol (Kim et al., 2010; Woo et al., 2016). Briefly, *E. coli* W (ATCC 1105) (Burkholder, 1951) was subjected to KAN-2 transposon insertion (Epicentre, WI, USA), and the resulting mutants were screened by replica plating on M9 minimal medium with and without supplementation of the respective amino acid to identify the desired auxotrophic phenotypes.

Competent cells of the auxotrophic strains were prepared by repeated washing with ice-cold distilled water and transformed via electroporation (Gene Pulser Xcell™, Bio-Rad, CA, USA) with plasmid pTacFadLGBP-1 (Ap^r, fadL, pTac99A derivative, *fadL*, GBP, 6.9 kb) for surface display of the GBP (Park et al., 2009). Transformants were selected on LB agar containing ampicillin (50 μg/mL), grown overnight in LB medium at 37 °C, and preserved as glycerol stocks at −70 °C. Using this protocol, ten GBP-expressing amino acid auxotrophs were constructed: Arg_GBP, His_GBP, Ile_GBP, Leu_GBP, Lys_GBP, Met_GBP, Phe_GBP, Thr_GBP, Trp_GBP, and Val_GBP. Surface display of GBP on the outer membrane was confirmed by 12 % (w/v) SDS-PAGE following standard membrane fractionation procedures (Woo et al., 2016).

2.2. Synthesis and characterization of AuNPs

Gold nanoparticles (AuNPs) were synthesized via citrate reduction, as previously described (Sugikawa et al., 2016). An aqueous solution of gold(III) chloride trihydrate (1 mM, 20 mL) was brought to a vigorous boil under continuous stirring, followed by the rapid addition of trisodium citrate (38.8 mM, 2 mL). The mixture was boiled for an additional 30 min, resulting in the formation of a deep-red colloidal solution. The solution was then cooled to room temperature and stored at 4 °C, yielding AuNPs at a final concentration of 13 nM. The synthesized AuNPs were characterized by transmission electron microscopy (TEM; FEI Tecnai, Japan) and energy-dispersive X-ray spectroscopy (EDS).

2.3. Cell-based colorimetric detection of amino acids

Auxotrophic strains were cultured overnight at 37 °C in LB medium supplemented with ampicillin and kanamycin (50 μg/mL each). Cells were harvested by centrifugation (8000×*g*, 3 min, 4 °C), washed with M9 medium, and resuspended to a final density of 1×10^7 cells in 50 μL per well of a transparent 96-well plate. Each well was then supplemented with 50 μL of a sample solution containing cyanocobalamin (1 nM), isopropyl-β-D-thiogalactopyranoside (IPTG; 1 mM), and target amino acids prepared in a standard amino acid cocktail simulating human blood composition (Liu et al., 2019; Woo et al., 2016). Typically, the amino acid cocktail contains (in μM): alanine (300), arginine (40), asparagine (60), aspartate (3), cysteine (45), glutamine (500), glutamate (50), glycine (220), histidine (65), isoleucine (65), leucine (100), lysine (180), methionine (20), phenylalanine (50), serine (100), threonine (120), tyrosine (60), tryptophan (20), valine (220), and proline (200). In each assay, the target amino acid was spiked into the cocktail to achieve the desired concentration. Following a 4-h incubation at 37 °C, the cells were washed twice with M9 medium and resuspended in 50 μL of fresh M9. AuNPs (5 nM, 100 μL per well) were then added to each well. The resulting pink-to-blue color shift, induced by target amino acid-triggered AuNP aggregation, was quantitatively evaluated by measuring the absorbance ratio at 700 nm and 562 nm (A_{700}/A_{562}) using a Synergy H1 microplate reader (BioTek, VT, USA). The limit of detection (LOD) value was calculated using the equation: $LOD = 3\sigma/S$, where σ is the standard deviation of the blank signal and S is the slope of the corresponding calibration curve.

For specificity testing, twenty wells of a 96-well plate were prepared with the same auxotrophic strain, and twenty different amino acid solutions (100 μM each) were individually added. The wells were then processed according to the procedure described above. Sensitivity and linearity assays were performed using serial dilutions of amino acids with maximum concentrations as follows: arginine, histidine, leucine, lysine, methionine, phenylalanine, and threonine (50 μM); isoleucine (25 μM); and tryptophan and valine (100 μM). Each assay was conducted according to the procedure described above.

2.4. Amino acid quantification from dried spot specimens

Blank filter paper disks (Whatman 903, Bio-Rad) were spotted with 20 μL of amino acid solutions (phenylalanine, methionine, and leucine) and dried at room temperature. Amino acids were extracted using 3 % trichloroacetic acid for 1 h at room temperature. The extracted solutions (30 μL) were then mixed with 90 μL of assay buffer containing 4 × M9 medium, sodium bicarbonate (1 M), cyanocobalamin (100 nM), and IPTG (100 mM), followed by analysis according to the standard assay procedure. Assay precision and reproducibility were evaluated by calculating recovery rates [% = (measured value/expected value) × 100] and coefficients of variation [CV % = (standard deviation/mean) × 100].

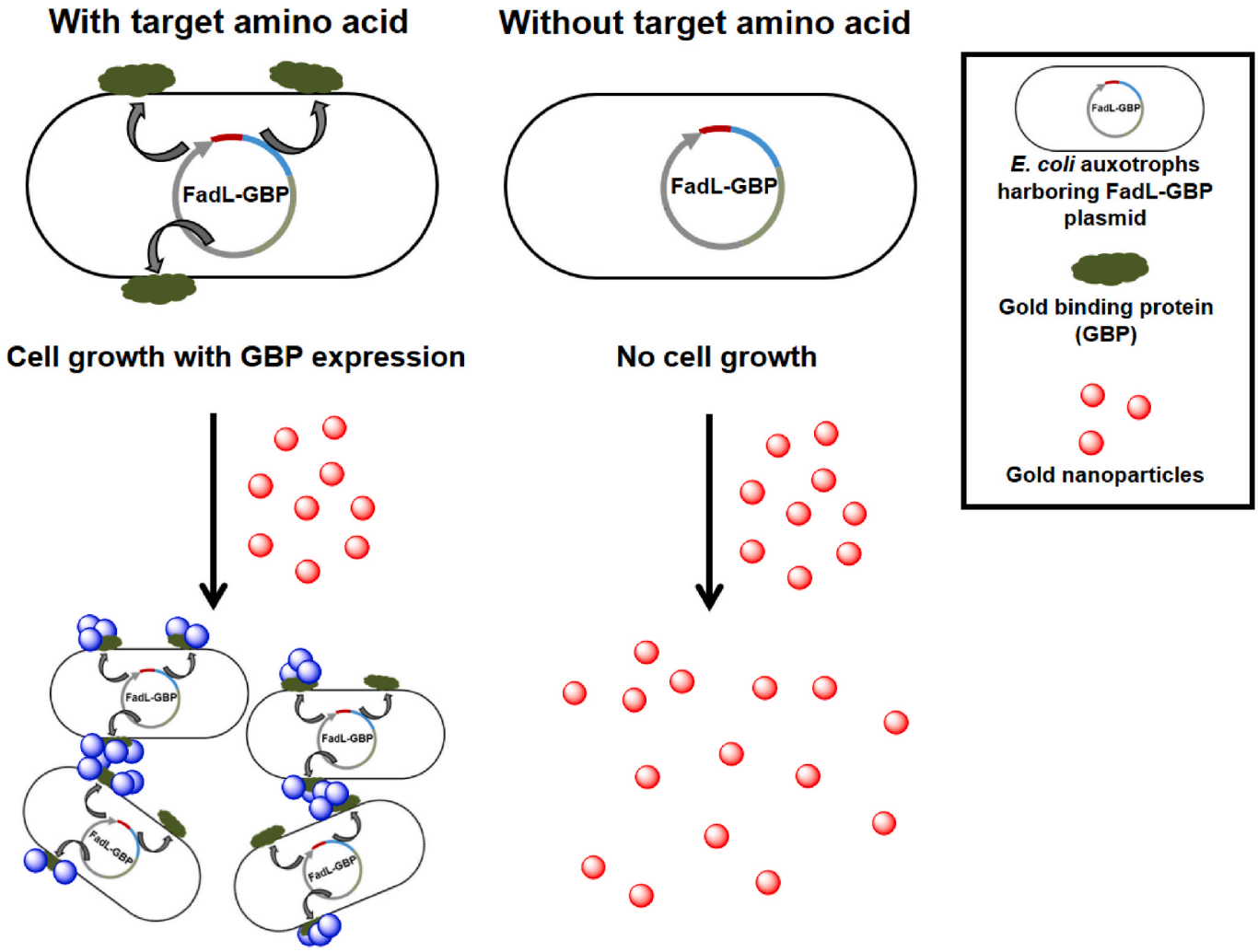

Fig. 1. Scheme of a colorimetric strategy for quantifying amino acids using *E. coli* auxotrophs displaying gold-binding proteins. (For interpretation of the references to color in this figure legend, the reader is referred to the Web version of this article.)

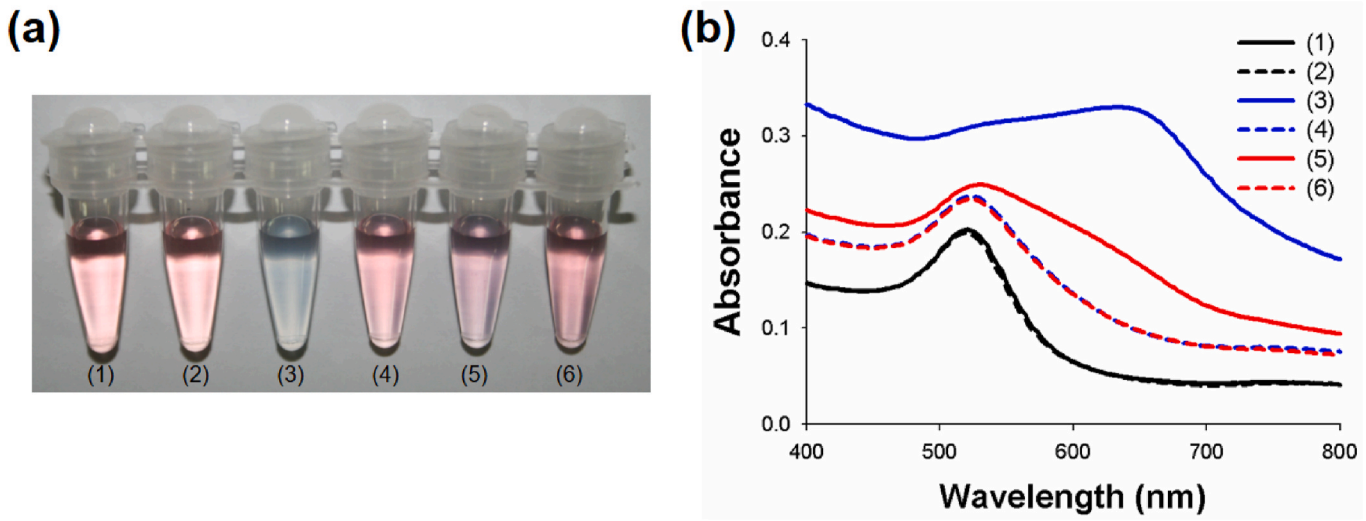

Fig. 2. Target-induced colorimetric transition via AuNP aggregation mediated by Met_GBP. (a) Real photographs and (b) their corresponding absorbance spectra. Sample specifications: (1) Free AuNPs, (2) AuNPs dispersed in M9 media, (3) Met_GBP incubated with Met, (4) Met_GBP incubated without Met, (5) Met auxotroph incubated with Met, (6) Met auxotroph incubated without Met.

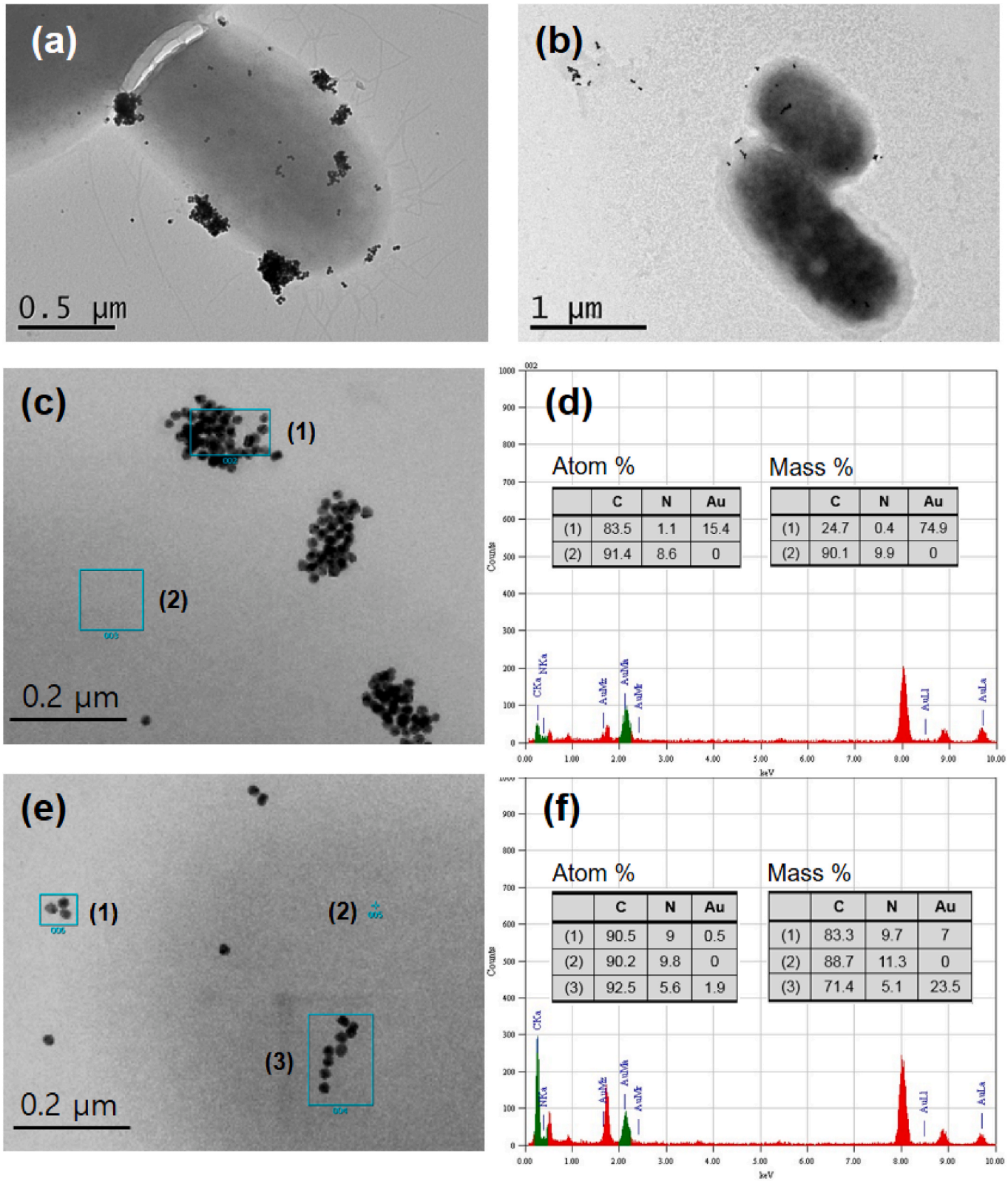

Atom %	C	N	Au
(1)	83.5	1.1	15.4
(2)	91.4	8.6	0

Mass %	C	N	Au
(1)	24.7	0.4	74.9
(2)	90.1	9.9	0

Atom %	C	N	Au
(1)	90.5	9	0.5
(2)	90.2	9.8	0
(3)	92.5	5.6	1.9

Mass %	C	N	Au
(1)	83.3	9.7	7
(2)	88.7	11.3	0
(3)	71.4	5.1	23.5

Fig. 3. Confirmation of methionine-induced AuNP aggregation on Met_GBP. TEM images illustrate the morphological characteristics of AuNPs incubated with Met_GBP cells either expressing GBP in the presence of methionine (a) or lacking GBP expression in the absence of methionine (b). EDS spectra and the corresponding atomic and mass ratios are shown for Met_GBP cells with GBP display (c, d) and without GBP display (e, f). Methionine concentration: 100 μM.

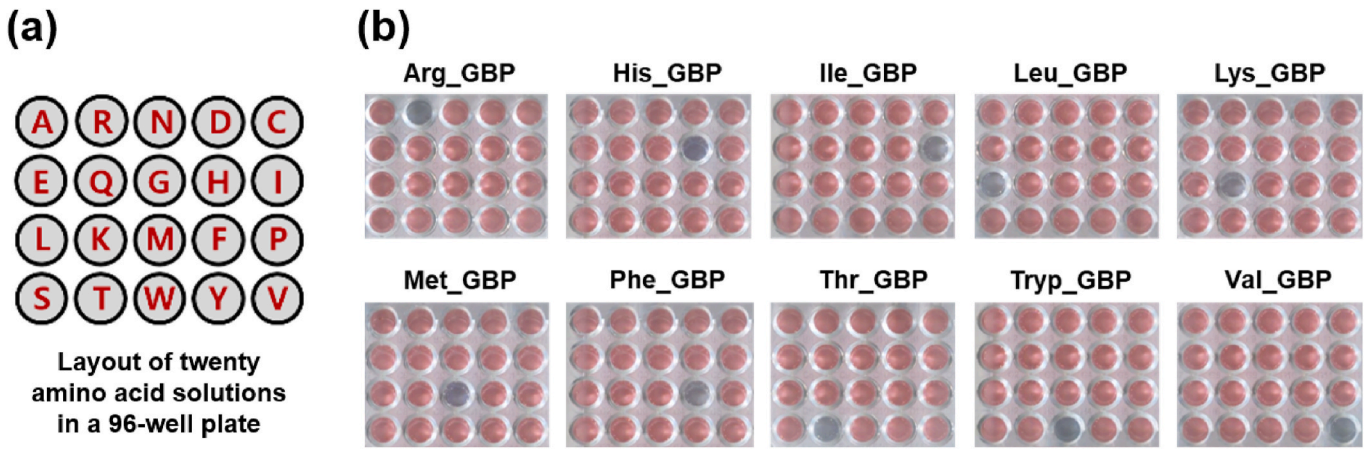

Fig. 4. Specificity assessment for the detection of ten essential amino acids. (a) Twenty different amino acid solutions were individually added to separate wells of a 96-well plate. (b) Each set of twenty wells was loaded with a single *E. coli* auxotroph and subjected to the colorimetric assay. The label above each image indicates the corresponding auxotrophic strain loaded.

3. Results and discussion

3.1. Colorimetric detection of amino acids via AuNP aggregation induced by GBP-displaying E. coli auxotrophs

Engineered *E. coli*-based biosensors offer notable advantages, including simplicity and cost-effectiveness. However, conventional systems often rely on specialized instrumentation to detect luminescence, fluorescence, or SPR signals generated from reporter gene expression associated with cell growth (Cevenini et al., 2016; Gupta et al., 2019; Jiang et al., 2015; Liu et al., 2014). To address these limitations, we developed a cell-based biosensor that retains these advantages while enabling amino acid detection through a visually observable color change.

Our system employs *E. coli* auxotrophs genetically engineered to display GBPs on their surface in the presence of specific amino acids. To enable detection of all ten essential amino acids, namely arginine, histidine, isoleucine, leucine, lysine, methionine, phenylalanine, threonine, tryptophan, and valine, we modified previously established auxotrophic strains (Kim et al., 2014) by introducing the plasmid pTacFadLGBP-1 into each. This plasmid encodes a FadL-GBP fusion protein under the control of the Tac promoter, allowing GBP to be expressed on the cell surface only when the corresponding amino acid is available. Successful surface expression of the fusion protein was confirmed by membrane fraction analysis (data not shown). Because each auxotroph can grow only when supplemented with its specific amino acid, GBP expression is proportional to the amino acid concentration in the sample. We hypothesized that the surface-localized GBP would bind to AuNPs, triggering their aggregation and resulting in a visible pink-to-blue color shift. This AuNP aggregation-based signal enables both qualitative and quantitative detection of essential amino acids without requiring advanced instrumentation (Fig. 1).

To validate the concept of colorimetric detection, we employed the Met_GBP strain as a model system. A distinct blue color appeared only in samples containing Met_GBP cells incubated with methionine (100 μM), indicating successful aggregation of AuNPs. In contrast, control samples including free AuNPs, AuNPs in M9 medium, Met_GBP without methionine, the Met auxotroph with methionine (100 μM), and the Met auxotroph without methionine remained pink with no observable color change (Fig. 2a). These visual results were supported by spectrophotometric analysis, which revealed characteristic absorbance peak shifts consistent with AuNP aggregation (Fig. 2b). Notably, minor spectral variations were observed in samples 4, 5, and 6, likely due to the presence of bacterial cells in the mixtures. The cell surface presents various functional groups (e.g., amine, carboxyl, and thiol moieties) that can weakly interact with AuNPs, resulting in marginal nonspecific adsorption and a subtle redshift (Woo et al., 2016; Tian et al., 2021). Samples 4 and 6 contained bacterial cells (Met_GBP and Met auxotrophs, respectively) without methionine supplementation, leading to no cell growth or GBP expression but still causing slight perturbations in the absorbance signal. In contrast, the Met auxotroph supplemented with methionine (sample 5) exhibited a somewhat larger shift due to increased cell density after growth activation, although the absence of GBP expression prevented specific AuNP aggregation. Similar minor shifts were also noted for other amino-acid systems (Fig. S1), verifying that these effects are nonspecific and negligible under practical assay conditions. Importantly, this minor perturbation phenomenon occurs only at relatively high amino acid concentrations and is negligible at low concentrations, thereby minimizing potential interference in practical diagnostic applications.

TEM further confirmed the presence of aggregated AuNPs on the surface of Met_GBP cells treated with methionine (Fig. 3a), while no such aggregation was observed in the Met auxotroph lacking GBP expression (Fig. 3b). In addition, EDS analysis showed a higher gold signal in Met_GBP samples exposed to methionine (Fig. 3c through 3f), further validating the specificity of the interaction. Collectively, these results demonstrate that GBP expression on the bacterial surface, which is regulated by auxotrophic growth in response to amino acid availability, induces AuNP aggregation and enables colorimetric detection of the target amino acid.

3.2. Specificity and quantitative response characteristics of GBP-displaying auxotrophs

To verify the specificity of the system, we evaluated ten *E. coli* auxotrophs engineered to display GBPs, each designed to respond to a distinct essential amino acid: arginine, histidine, isoleucine, leucine, lysine, methionine, phenylalanine, threonine, tryptophan, and valine. For each strain, twenty wells of a 96-well plate were loaded with the same auxotroph, and twenty different amino acid solutions (100 μM each) were individually added to the wells, as illustrated in Fig. 4a. The sequence of the twenty amino acid solutions used in the assay was as follows: A (alanine), R (arginine), N (asparagine), D (aspartic acid), C (cysteine), E (glutamic acid), Q (glutamine), G (glycine), H (histidine), I (isoleucine), L (leucine), K (lysine), M (methionine), F (phenylalanine), P (proline), S (serine), T (threonine), W (tryptophan), Y (tyrosine), and V (valine), arranged from left to right and top to bottom.

After incubation, the cells were washed with M9 medium to remove residual cysteine, which is known to induce nonspecific AuNP aggregation (Apyari et al., 2018). Upon the addition of AuNPs, a rapid color

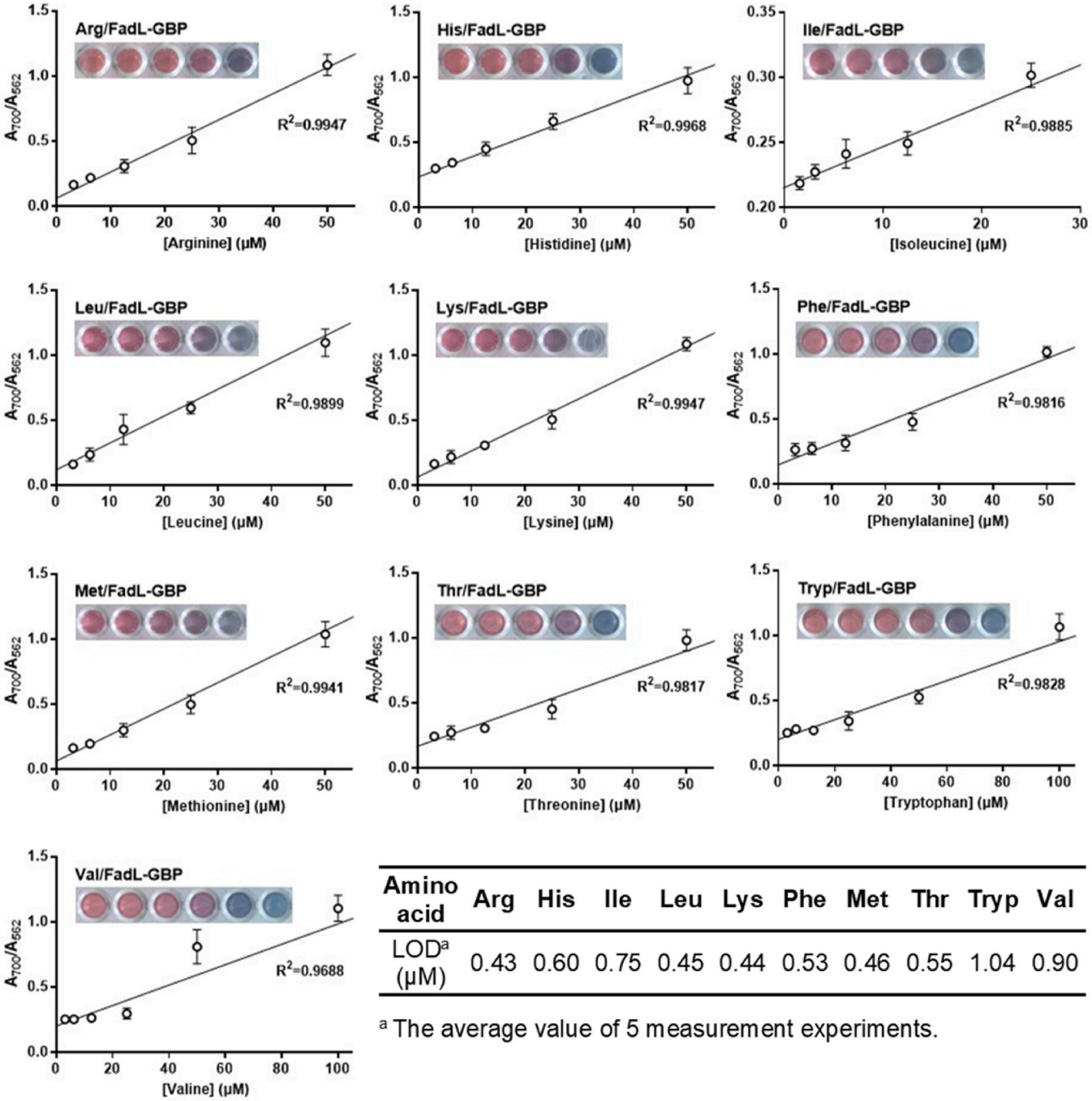

Amino acid	Arg	His	Ile	Leu	Lys	Phe	Met	Thr	Tryp	Val
LOD[a] (μM)	0.43	0.60	0.75	0.45	0.44	0.53	0.46	0.55	1.04	0.90

[a] The average value of 5 measurement experiments.

Fig. 5. Linear correlation between target amino acid concentrations and colorimetric responses, with corresponding LOD values for ten essential amino acids.

shift (within 1 min) was observed exclusively in wells where the auxotrophs were exposed to their corresponding amino acids (Fig. 4b). Notably, all ten GBP-displaying auxotrophs exhibited a clear blue color only in response to their target amino acid, while no color change was observed in any of the mismatched combinations. This result highlights the high level of molecular recognition achieved by the system, in which GBP expression is tightly regulated by auxotroph-specific growth and functions as a reliable trigger for AuNP aggregation. The robustness and consistency of this colorimetric response across all ten strains support the specificity and scalability of this approach for multiplexed amino acid detection. Spectrophotometric analysis of the absorbance ratio (A_{700}/A_{562}) further confirmed AuNP binding and aggregation on the bacterial surface (Fig. S2), validating the high specificity of this detection system. These findings underscore the high specificity of each GBP-displaying *E. coli* auxotroph toward its cognate amino acid and highlight the feasibility of extending this concept into a multiplexed array format for simultaneous detection of multiple amino acids.

To evaluate the quantitative performance of the system, we investigated the linearity of the response across a range of amino acid concentrations using all ten GBP-displaying *E. coli* auxotrophs. Initial spectral analysis using Met_GBP and Leu_GBP confirmed concentration-dependent peak shifts in absorbance (Fig. S3). Subsequently, the absorbance ratio (A_{700}/A_{562}) was measured as a function of the corresponding amino acid concentration for each strain. All auxotrophs exhibited strong linear correlations, with R^2 values exceeding 0.96 (Fig. 5), and detection limits in the low micromolar to sub-micromolar range, indicating high sensitivity and robustness of the assay. Specifically, the LOD values for arginine, histidine, isoleucine, leucine, lysine,

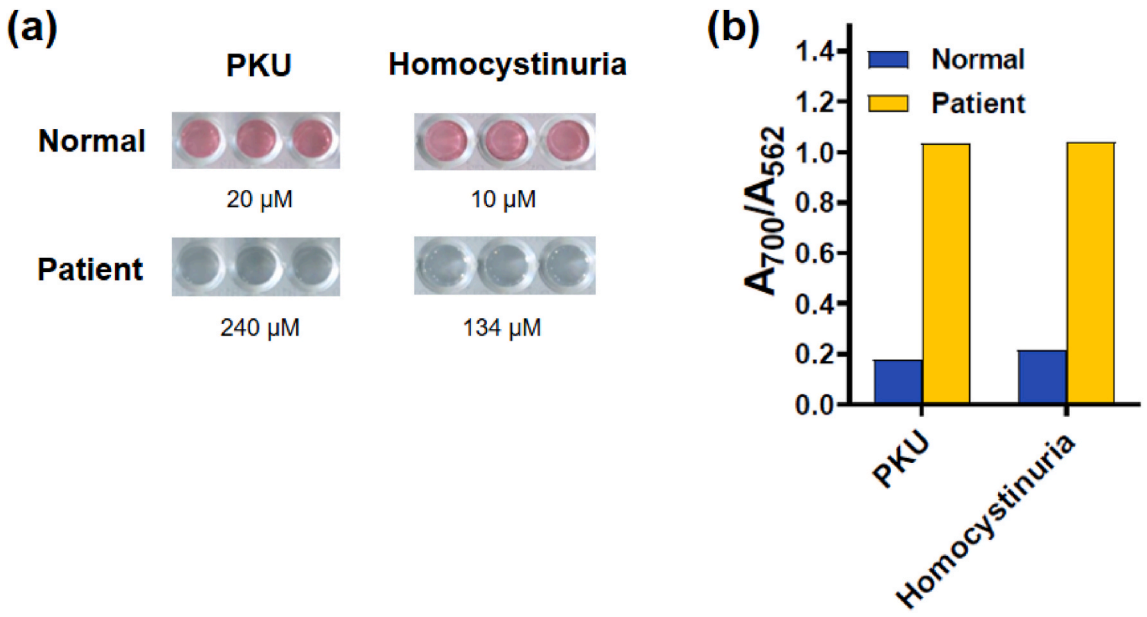

Fig. 6. Diagnosis of PKU and homocystinuria using clinical dried spot specimens spiked with normal and pathological levels of Phe and Met. (a) Photographs of colorimetric responses and (b) their corresponding A_{700}/A_{562} value.

phenylalanine, methionine, threonine, tryptophan, and valine were determined to be 0.43, 0.60, 0.75, 0.45, 0.44, 0.53, 0.46, 0.55, 1.04, and 0.90 μM, respectively. These results demonstrate that the platform is well-suited for detecting clinically relevant amino acid abnormalities associated with nutritional deficiencies and inborn errors of metabolism. Although fluorescence-, luminescence-, SPR-, and Raman-based biosensing methods generally provide higher analytical sensitivity, they typically require complex labeling procedures and expensive detection instrumentation, limiting their practicality for point-of-care applications. In contrast, the colorimetric AuNP-based strategy developed here achieves comparable sub-micromolar sensitivity through a simple, label-free mechanism, while offering superior accessibility, scalability, and suitability for decentralized clinical diagnostics. Moreover, compared with conventional analytical techniques such as tandem mass spectrometry (MS/MS) and HPLC, this approach provides distinct advantages in terms of shorter analysis time, lower cost, and reduced operational complexity (Table S1).

3.3. *Clinical application of GBP-displaying auxotrophs for diagnosing aminoacidopathies*

Abnormal blood amino acid concentrations are indicative of various inherited metabolic disorders that affect amino acid metabolism or transport (Garg and Dasouki, 2006; Yahyaoui and Pérez-Frías, 2019). Early detection of such disorders through newborn screening is critical to prevent irreversible physiological damage. In this study, we focused on three representative aminoacidopathies: phenylketonuria (PKU, characterized by elevated phenylalanine), homocystinuria (elevated methionine), and maple syrup urine disease (MSUD, characterized by elevated isoleucine, leucine, and valine). For MSUD, leucine was selected as a representative biomarker among the three branched-chain amino acids.

To validate the assay's diagnostic capability, the system was first applied to differentiate PKU and homocystinuria, both of which can be diagnosed using a single amino acid marker (phenylalanine and methionine, respectively). Dried spot samples containing either normal or elevated levels were analyzed, and the corresponding A_{700}/A_{562} absorbance ratios, together with visual inspection, clearly confirmed the assay's effectiveness (Fig. 6a and b). A distinct pink-to-blue color change was observed in patient-level samples, along with significantly increased absorbance ratios compared to normal samples.

Table 1
Accuracy and precision in quantifying phenylalanine, methionine, and leucine from dried spot specimens using GBP-expressing *E. coli* auxotrophs.

	Phe		Met		Leu	
	Normal	Patient	Normal	Patient	Normal	Patient
Added (μM)	20.0	240.0	10.0	134.0	50.0	422.0
Measured[a] (μM)	20.2	243.5	10.1	133.4	49.4	424.1
SD	0.8	3.4	0.2	2.4	1.3	5.1
CV (%)	3.9	1.4	1.8	1.8	2.6	1.2
Recovery (%)	100.9	101.5	100.8	99.5	98.9	100.5

[a] The average value of 5 measurement experiments.

Following the qualitative validation, we evaluated the quantitative diagnostic performance of our colorimetric biosensing system by detecting phenylalanine, methionine, and leucine in clinical dried spot specimens. The GBP-displaying *E. coli* auxotrophs reliably distinguished and quantified both normal and patient-level concentrations for each target amino acid (Table 1). Elevated concentrations exceeding clinical thresholds, namely phenylalanine (>200 μM), methionine (>100 μM), and leucine (>300 μM), were successfully detected with high analytical precision (coefficients of variation <4 %) and excellent recovery rates ranging from 98 % to 102 % across all tested samples. Furthermore, to emphasize the broader applicability of the developed platform, the clinical relevance and typical pathological concentration ranges of all ten essential amino acids were summarized (Table S2). With detection limits in the low-micromolar range, our system offers sufficient sensitivity to identify clinically significant deviations across all essential amino acids.

These results demonstrate that the auxotroph-based colorimetric assay provides a robust, low-complexity, and clinically relevant platform for diagnosing amino acid-related metabolic disorders, particularly in formats compatible with newborn screening. Nonetheless, several challenges need to be addressed to advance its translational potential. Specifically, assay speed is constrained by the growth-dependent GBP expression step, the long-term stability of both engineered cells and AuNPs requires improvement, and nonspecific matrix effects from complex biological samples may affect performance. To overcome these limitations, potential strategies include: (i) genetic optimization to

enhance GBP expression and accelerate cellular response; (ii) lyophilization or encapsulation approaches to extend shelf life (Ahn et al., 2021); and (iii) the use of stabilizers to suppress unintended AuNP aggregation. Implementation of these improvements is expected to further enhance the assay's sensitivity, reproducibility, and clinical applicability.

4. Conclusions

This study introduces the first colorimetric biosensing platform for amino acid detection and aminoacidopathy diagnosis based on *E. coli* auxotrophs expressing GBP. By engineering bacterial cells to display GBP on surface in proportion to target amino acid concentrations, we successfully achieved target-induced aggregation of AuNPs, consequently resulting in a rapid and visible pink-to-blue color change. The system demonstrated excellent specificity, linearity, and sensitivity, achieving detection limits in the micromolar range with excellent resistance to interference from complex physiological matrices. Clinically relevant levels of phenylalanine, methionine, and leucine were successfully quantified from dried spot specimens, allowing accurate differentiation between normal and pathological concentrations. This enabled reliable diagnosis of PKU, homocystinuria, and MSUD without the need for specialized instrumentation or advanced analytical infrastructure. The assay provides a simple, scalable, and cost-effective alternative to conventional amino acid analysis while maintaining compatibility with standard spectrophotometric quantification when required.

CRediT authorship contribution statement

Hee Tae Ahn: Writing – original draft, Investigation, Conceptualization. **Byung Jo Yu:** Investigation, Conceptualization. **Thinh Viet Dang:** Writing – original draft, Investigation. **Soobin Lee:** Validation, Investigation. **In Seung Jang:** Validation, Investigation. **Dong Hoon Lee:** Investigation, Conceptualization. **Tae Jung Park:** Validation. **Moon Il Kim:** Writing – review & editing, Supervision, Conceptualization. **Hyun Gyu Park:** Writing – review & editing, Supervision, Conceptualization.

Declaration of competing interest

The authors declare that they have no known competing financial interests or personal relationships that could have appeared to influence the work reported in this paper.

Acknowledgment

This work was supported by the Technology Innovation Program 'Development of Korea-led K-Sensor Technology for Market Leadership' (Development of Fully Integrated Electrochemical Microfluidic System for Ultra-sensitive and Rapid Multiplex-Diagnosis of Respiratory Tract Infections, RS-2024-00400234) funded By the Ministry of Trade, Industry and Energy (MOTIE, Korea) and by the Korea Planning & Evaluation Institute of Industrial Technology (KEIT) and MOTIE (RS-2023-00235283). This research was also supported by National Research Foundation of Korea (NRF) grant funded by the Korea government (MSIT) (RS-2023-00218543). This work was supported by a NRF grant funded by the Korean government (Ministry of Science and ICT [RS-2023-NR077205]) and the Basic Science Research Program through the NRF funded by the Ministry of Education (RS-2021-NR060117).

Appendix B. Supplementary data

Supplementary data to this article can be found online at https://doi.org/10.1016/j.bios.2025.118182.

Data availability

Data will be made available on request.

References

Ahn, H.T., Jang, I.S., Dang, T.V., Kim, Y.H., Lee, D.H., Choi, H.S., Yu, B.J., Kim, M.I., 2021. Effective cryopreservation of a bioluminescent auxotrophic *escherichia coli*-based amino acid array to enable long-term ready-to-use applications. Biosensors 11 (8), 252.
Aliu, E., Kanungo, S., Arnold, G.L., 2018. Amino acid disorders. Ann. Transl. Med. 6 (24), 471.
Apyari, V.V., Arkhipova, V.V., Isachenko, A.I., Volkov, P.A., Dmitrienko, S.G., Torocheshnikova, I.I., 2018. Label-free gold nanoparticle-based sensing of cysteine: new peculiarities and prospects. Sensor. Actuator. B Chem. 260, 953–961.
Bertels, F., Merker, H., Kost, C., 2012. Design and characterization of auxotrophy-based amino acid biosensors. PLoS One 7 (7), e41349.
Bouza, M., Foest, D., Brandt, S., García-Reyes, J.F., Franzke, J., 2024. Enhanced compound analysis using reactive paper spray mass spectrometry: leveraging schiff base reaction for amino acid detection. Anal. Chem. 96 (13), 5289–5297.
Burkholder, P.R., 1951. Determination of vitamin B12 with a mutant strain of *Escherichia coli*. Science 114 (2966), 459–460.
Cevenini, L., Calabretta, M.M., Tarantino, G., Michelini, E., Roda, A., 2016. Smartphone-interfaced 3D printed toxicity biosensor integrating bioluminescent "sentinel cells.". Sensor. Actuator. B Chem. 225, 249–257.
Chen, T., Lu, D., Xu, F., Ji, W., Zhan, X., Gao, X., Qiu, W., Zhang, H., Liang, L., Gu, X., 2023. Newborn screening of maple syrup urine disease and the effect of early diagnosis. Clin. Chim. Acta 548, 117483.
Chung, T.H., Dhar, B.R., 2021. Paper-based platforms for microbial electrochemical cell-based biosensors: a review. Biosens. Bioelectron. 192, 113485.
Garg, U., Dasouki, M., 2006. Expanded newborn screening of inherited metabolic disorders by tandem mass spectrometry: clinical and laboratory aspects. Clin. Biochem. 39 (4), 315–332.
Giordano, G., Gucciardi, A., Pirillo, P., Naturale, M., 2019. Quantification of underivatized amino acids on dry blood spot, plasma, and urine by HPLC-ESI-MS/MS. In: Alterman, M.A. (Ed.), Amino Acid Analysis: Methods Protocols. Humana, New York, New York, pp. 153–172.
Gupta, N., Renugopalakrishnan, V., Liepmann, D., Paulmurugan, R., Malhotra, B.D., 2019. Cell-based biosensors: recent trends, challenges and future perspectives. Biosens. Bioelectron. 141, 111435.
Han, H.-S., Ahn, E., Park, E.S., Huh, T., Choi, S., Kwon, Y., Choi, B.H., Lee, J., Choi, Y.H., Jeong, Y.L., 2023. Impaired BCAA catabolism in adipose tissues promotes age-associated metabolic derangement. Nat. Aging 3 (8), 982–1000.
Häusler, R.E., Ludewig, F., Krueger, S., 2014. Amino acids–a life between metabolism and signaling. Plant Sci. 229, 225–237.
Hou, Y., Yin, Y., Wu, G., 2015. Dietary essentiality of "nutritionally non-essential amino acids" for animals and humans. Exp. Biol. Med. 240 (8), 997–1007.
Jiang, D., Zhu, P., Jiang, H., Ji, J., Sun, X., Gu, W., Zhang, G., 2015. Fluorescent magnetic bead-based mast cell biosensor for electrochemical detection of allergens in foodstuffs. Biosens. Bioelectron. 70, 482–490.
Kang, C., Shrestha, K.L., Kwon, S., Park, S., Kim, J., Kwon, Y., 2022. Intein-mediated protein engineering for cell-based biosensors. Biosensors 12 (5), 283.
Kannappan, S., Ramisetty, B.C.M., 2022. Engineered whole-cell-based biosensors: sensing environmental heavy metal pollutants in water—a review. Appl. Biochem. Biotechnol. 1–27.
Kaur, J., Rangra, N.K., Chawla, P.A., 2023. A comprehensive review on recent trends in amino acids detection through analytical techniques. Sep. Sci. Plus 6 (11), 2300040.
Kilgore, M.B., Platis, D., Lim, T., Isenberg, S., Pickens, C.A., Cuthbert, C., Petritis, K., 2023. Development of a universal second-tier newborn screening LC–MS/MS method for amino acids, lysophosphatidylcholines, and organic acids. Anal. Chem. 95 (6), 3187–3194.
Kim, M.I., Park, T.J., Heo, N.S., Woo, M.-A., Cho, D., Lee, S.Y., Park, H.G., 2014. Cell-based method utilizing fluorescent Escherichia coli auxotrophs for quantification of multiple amino acids. Anal. Chem. 86 (5), 2489–2496.
Kim, M.I., Yu, B.J., Woo, M.-A., Cho, D., Dordick, J.S., Cho, J.H., Choi, B.-O., Park, H.G., 2010. Multiplexed amino acid array utilizing bioluminescent Escherichia coli auxotrophs. Anal. Chem. 82 (10), 4072–4077.
Liu, Q., Wu, C., Cai, H., Hu, N., Zhou, J., Wang, P., 2014. Cell-based biosensors and their application in biomedicine. Chem. Rev. 114 (12), 6423–6461.
Liu, Z., Tu, M.-J., Zhang, C., Jilek, J.L., Zhang, Q.-Y., Yu, A.-M., 2019. A reliable LC-MS/MS method for the quantification of natural amino acids in mouse plasma: method validation and application to a study on amino acid dynamics during hepatocellular carcinoma progression. J. Chromatogr. B 1124, 72–81.
Lu, X., Ye, Y., Zhang, Y., Sun, X., 2021. Current research progress of mammalian cell-based biosensors on the detection of foodborne pathogens and toxins. Crit. Rev. Food Sci. Nutr. 61 (22), 3819–3835.
Matuszewska, E., Matysiak, J., Kałużny, Ł., Walkowiak, D., Plewa, S., Duś-Żuchowska, M., Rzetecka, N., Jamka, M., Klupczyńska-Gabryszak, A., Piorunek, M., 2024. Amino acid profile alterations in phenylketonuria: implications for clinical practice. Metabolites 14 (7), 397.
Park, T.J., Zheng, S., Kang, Y.J., Lee, S.Y., 2009. Development of a whole-cell biosensor by cell surface display of a gold-binding polypeptide on the gold surface. FEMS Microbiol. Lett. 293 (1), 141–147.

Shykholeslami, A., Ghavami, R., Rasouli, Z., 2022. Fully united, easy, and economical sensor array for newborn babies' amino acids monitoring: identification of amino acids in healthy and unhealthy with PKU newborn babies. J. Pharm. Biomed. Anal. 213, 114683.

Sugikawa, K., Kadota, T., Yasuhara, K., Ikeda, A., 2016. Anisotropic self-assembly of citrate-coated gold nanoparticles on fluidic liposomes. Angew. Chem.-Int. Edit. 55 (12), 4059–4063.

Tian, E.K., Wang, Y., Ren, R., Zheng, W., Liao, W., 2021. Gold nanoparticle: recent progress on its antibacterial applications and mechanisms. J. Nanomater. 1, 2501345.

Woo, M.-A., Park, J.H., Cho, D., Sim, S.J., Kim, M.I., Park, H.G., 2016. A whole-cell surface plasmon resonance sensor based on a leucine auxotroph of *Escherichia coli* displaying a gold-binding protein: usefulness for diagnosis of maple syrup urine disease. Anal. Chem. 88 (5), 2871–2876.

Woo, M.-A., Kim, M.I., Cho, D., Park, H.G., 2013. Cell-based galactosemia diagnosis system based on a galactose assay using a bioluminescent *Escherichia coli* array. Anal. Chem. 85 (22), 11083–11089.

Woo, M.-A., Kim, M.I., Yu, B.J., Cho, D., Kim, N.-J., Cho, J.H., Choi, B.-O., Chang, H.N., Park, H.G., 2011. Cell-based quantification of homocysteine utilizing bioluminescent *Escherichia coli* auxotrophs. Anal. Chem. 83 (8), 3089–3095.

Xie, C., Chen, Y., Wang, X., Song, Y., Shen, Y., Diao, X., Zhu, L., Wang, J., Cai, Z., 2022. Chiral derivatization-enabled discrimination and on-tissue detection of proteinogenic amino acids by ion mobility mass spectrometry. Chem. Sci. 13 (47), 14114–14123.

Yahyaoui, R., Pérez-Frías, J., 2019. Amino acid transport defects in human inherited metabolic disorders. Int. J. Mol. Sci. 21 (1), 119.

Zhang, M., Tang, C., Wang, Z., Chen, S., Zhang, D., Li, K., Sun, K., Zhao, C., Wang, Y., Xu, M., 2024. Real-time detection of 20 amino acids and discrimination of pathologically relevant peptides with functionalized nanopore. Nat. Methods 21 (4), 609–618.